Carbon 175 (2021) 403–412

Contents lists available at ScienceDirect

Carbon

journal homepage: www.elsevier.com/locate/carbon

3-D structured porous carbons with virtually any shape from whey powders

Raúl Llamas-Unzueta [a], J. Angel Menéndez [a, *], Luis A. Ramírez-Montoya [a], Jaime Viña [b], Antonio Argüelles [c], Miguel A. Montes-Morán [a]

[a] Instituto de Ciencia y Tecnología del Carbono, INCAR-CSIC, c/Francisco Pintado Fe 26, 33011, Oviedo, Spain
[b] Department of Materials Science and Metallurgical Engineering, University of Oviedo, Polythecnic School of Engineering, 33203, Gijón, Spain
[c] Department of Construction and Manufacturing Engineering, University of Oviedo, Polytechnic School of Engineering, 33203, Gijón, Spain

ARTICLE INFO

Article history:
Received 2 December 2020
Received in revised form
3 January 2021
Accepted 7 January 2021
Available online 12 January 2021

Keywords:
Carbon monoliths
Porous carbon
Whey

ABSTRACT

The conventional carbonisation (450-1000 °C) of whey powders gives totally unexpected results in terms of the mechanical integrity of the resulting carbons. Pieces of different geometries can be easily prepared by pouring the powders loosely into a mould. This green precursor adopts the shape of the predesigned mould at relatively low temperatures (120-150 °C) through the sintering of the whey particles surfaces. The shape of the pre-conformed pieces is preserved at least up to 1000 °C under N_2 atmosphere, with a linear shrinkage of ca. 23%. The flexural strength and modulus of the resulting 3-D structured porous carbons are outstanding for a biomass derived carbon monolith, and their abrasiveness exceptionally low, similar to porous monoliths derived from phenolic resins. In addition, carbons obtained at temperatures above 800 °C develop a hierarchical porosity covering from micropores to macropores up to 400 μm granting high permeable structures. It is postulated that the presence of both lactose and whey proteins in whey powders is key for their atypical behaviour during carbonisation.

1. Introduction

Making porous carbons with a desired 3-D shape is not straightforward. Such 3-D structures offer several advantages over granular or powdered activated carbons, relying on a hierarchical porosity that combines transport pores (macropores) with the inherent porosity of carbons developed at the nanometer scale (micro and mesopores) [1–5]. There are indeed some industrial applications where 3-D structured porous carbons have found their niche including filters (e.g., for the abatement of volatile organic compounds, VOCs), or catalyst supports in heterogeneous catalytic reactors [6–8]. Moreover, in the age of the rise of additive manufacturing technologies [9,10], porous carbons with complex geometries are expected in new applications [11].

For the industrial applications already mentioned, 3-D structured porous carbons do not only require adequate textural properties but also mechanical properties are a must. In that sense, very interesting 3-D highly porous carbons, mainly carbon aerogels and carbon foams, obtained by elegant synthetic routes are out of the picture here [3,12,13]. Template carbons can also be prepared as monolithic structures but again with limited mechanical integrity [14].

Thus, leaving aside the preparation of carbon coated structures, there are currently two fundamental approaches to obtain 3-D structured porous carbons with acceptable mechanical properties [6]. Possibly the most explored path consists in the combination of porous (or not) carbon powders, granules or fibres with an appropriate binder that, after carbonisation (or activation), confers the mechanical stability [15–17]. This particular route has substantial drawbacks related to the use of binders, including the control of the porosity and of the mechanical properties of the resulting 3-D carbon materials [18,19]. The other alternative is much more rare and limited to the use of polymers or resins as precursors that overcomes the need for binders [19–22]. Specifically, the use of partially cured phenolic resins demonstrated the possibility of attaining porous carbons of the desired shape by extrusion or moulding. These porous carbon structures have superior mechanical properties [6,19].

This paper presents a green alternative to those phenolic derived carbons by using a sustainable precursor -whey powders.

* Corresponding author.
E-mail address: angelmd@incar.csic.es (J.A. Menéndez).

https://doi.org/10.1016/j.carbon.2021.01.021

Whey is a liquid by-product in the manufacture of cheese and casein. Generally speaking, liquid whey contains an average of 6.5% of solids, of which almost 80% is lactose. Although the detailed composition of whey varies depending on the milk involved and its processing, liquid whey has a very high biochemical oxygen demand (BOD = 27–60 kg m^{-3}) [23], which strongly hampers its disposal. With dairy products volumes increasing year by year, whey management is a serious issue for dairy industries to fulfil environmental regulations. Thus, different biological and physicochemical treatments are nowadays available to reduce the impact of this by-product, with some of them also looking for its valorisation [23,24]. Amongst the latter ones, dehydration of whey by spray drying is possibly the most extended technology within big dairy companies that need to process huge amounts of liquid whey per year. The resulting product is known as whey powder and it normally contains less than 2.5% of remaining moisture. Whey powder is directed towards food market, mainly animal feed [25]. Still, whey powder marketing is limited by the fact that more than 75% of its composition is lactose. This disaccharide has little commercial value and strongly reduces the commercial applications of whey powders [24]. As a consequence, important amounts of whey powders end as food waste biomass [27–29].

The approach we are presenting here would then also offer a modest alternative for whey valorisation. Although most research on whey and whey powders valorisation is related, unsurprisingly, to Food Science and Technology, some researchers have explored the possibility of using those by-products to obtain materials. Some examples include the synthesis of foams from whey protein isolates [30], and the use of *Pseudomonas* spp. and other microorganisms to obtain bioplastics (i.e., polyhydroxyalkanoates) from liquid whey [31]. More specifically, in the field of carbon materials whey has been used aiming at the nitrogen enrichment of electrode materials for energy storage devices [32]. Hydrothermal treatment of whey has also been explored and carbonised powders with contents up to 65% of elemental C were obtained at fairy low temperatures (205 °C) [33].

This paper, however, describes for the first time the possibility of obtaining 3-D structured porous carbons with exceptional mechanical properties from whey powders. As it will be demonstrated, the making of these carbons resembles a sintering process in which whey powder particulates fuse to form the final carbon material.

2. Materials and methods

2.1. Materials

Whey powder was provided by a Spanish dairy company. A commercial Whey Protein Isolate (WPI, 80% of whey protein content from DOMYOS®) and α-lactose (monohydrate, >99.5% from MERCK) were used as reference materials.

2.2. Synthesis process

In a typical procedure, 10 g of powdered whey were used to fill moulds with different shapes. First, samples were heated in air in a lab oven at 20 °C min^{-1} up to 150 °C (HW150) for 2 h and then demoulded. Moulds used for this pre-conforming step include ceramic (alsint®), silicone and steel. The whey powders were simply poured loosely into the moulds. The demoulding process was free of sticking or cracking issues. The pre-conformed piece was then placed in a ceramic (alsint®) crucible and heat-treated in a tubular electric furnace. The carbonisation was carried out in an inert atmosphere of N_2 (100 ml min^{-1}) at temperatures between 450 °C and 1000 °C (PWtemperature). Heating ramps and dwell times were 10 °C min^{-1} and 1.5 h, respectively. It should be clear that, if the mould withstands temperature, whey derived carbons can be obtained in a one-step synthesis where the powders contained in the mould would be heated up in a furnace to the desired temperature under appropriate atmosphere.

2.3. Characterisation techniques

Organic (CHNSO) elemental analysis was carried out in LECO CHNS-932 and LECO VTF-900 microanalysers. Elemental analysis of other inorganic elements was carried out using inductively coupled plasma mass spectrometry (ICP-MS) in an Agilent 7700× apparatus, except for Cl determination for which an ion selective electrode (ISE) was used.

SEM micro photographs were obtained in a Quanta FEG 650 microscope. Samples were attached to an aluminium tap using conductive double-sided adhesive tape. No further coating was used.

N_2 adsorption isotherms were carried out in a Micromeritics Tristar II volumetric adsorption system at −196 °C. Before the measurement, samples were outgassed by heating at 120 °C under vacuum during 12 h. BET surface area was determined using the Brunauer-Emmett-Teller model, and micropore volumes were obtained from the Dubinin-Radushkevich model. Pore size distributions (PSD) were obtained from the N_2 adsorption branch using the DFT method.

The true density of the materials (ρ_{He}) was measured with a Micromeritics AccuPyc 1330 pycnometer, using He as the probe gas. Hg intrusion was performed in a Micromeritics AutoPore IV porosimeter up to a maximum operating pressure of 227 MPa. Small pieces (rectangular prisms of approx. 0.8 × 0.3 cm sides) were intruded by Hg. Apparent densities (ρ_{Hg}) and pore size distributions (pore sizes 4 10^{-3}-100 μm) were obtained from the intrusion curves. In both cases the samples were outgassed at 120 °C for 12 h before the analysis.

The point of zero charge (pH_{pzc}) of the 3-D structured porous carbons was determined after grinding (<0.212 mm) 250 mg of sample and preparing a suspension of the powders into a certain volume of distilled water. The suspension was kept closed and under continuous stirring. The pH was measured daily as the amount of water was increased. The pH_{pzc} value was obtained from the plateau of the pH variation curve [34].

Thermogravimetric analyses (TG) were carried out in a SDT Q600 thermobalance from TA instruments. 25 (±0.1) mg of whey powder were heated under 100 ml min^{-1} of N_2 at 10 °C/min. Quantities of lactose and WPI tested were adjusted to approx. their relative proportions in whey powders, i.e., 20 (±0.1) mg and 5 (±0.1) mg, respectively.

The intrinsic permeability of the 3-D structured porous carbons (k) was measured by passing an increasing gas flow (He) through the cylindrical axis of rods (10 mm length and diameter). The intrinsic permeability (k) is related to the gas volume flowing through the permeameter cross section (v_L), monolith length (L), gas viscosity (μ_{gas}), final pressure (P_L) and initial pressure (P_0), according to the Darcy's equation:

$$k = 2v_L L\mu_{gas}PL/(P0^2 - PL^2) \quad (1)$$

The flexural modulus and flexural strength of the whey-derived carbons were calculated from a 3-point bending test using prismatic specimens. The test conditions followed the recommendations of the BS EN843-1: 2006 standard corresponding to advanced technical ceramics. A Sinergy 5 kN electromechanical machine (MTS Systems Corporation) provided with a 100 N load cell was used. The crosshead speed was 0.5 mm min^{-1}. The distance between the centres of the two outer supports (L) was fixed at 40 mm.

Rectangular beams with nominal dimensions of 4 × 4 × 45 mm were tested. True values of the width (w; mm) and thickness (t; mm) of each specimen resulted from the average of 3 measurements taken along its length. Flexural strength (σ_f; MPa) was calculated from the maximum load (F; N) attained, according to:

$$\sigma_f = 3FL/2wt^2 \quad (2)$$

Flexural moduli (E_f; MPa) were calculated from the slope of the linear part of the load vs. displacement (Y; mm) curves, assuming the tested specimens were isotropic: $\Delta F/\Delta Y]$

$$\boldsymbol{E_f} = \frac{\boldsymbol{L^3}}{\boldsymbol{4wt^3}}[\Delta F/\Delta Y] \quad (3)$$

Values of flexural modulus and flexural strength reported for each material corresponded to the average of, at least, 11 tests.

Abrasion studies of the whey-derived carbons were carried out using 1 cm^3 cubes obtained by casting of whey powders at different temperatures. These cubes were subjected to a drum test adapted from the ISO 556 International Standard using a RETSCH MM400 ball mill. The cubes were placed into a stainless steel cylindrical drum 55 mm length and 26 mm diameter (inner dimensions) containing a stainless steel ball of 14 mm diameter. The drum was shaken at a frequency of 10 Hz for 60 s. After this, the broken pieces were classified, by sieving, into those rejected by a 5 mm sieve and those that passed through a 0.5 mm sieve, defining a cohesion index (Ic) or wt% of pieces ≥5 mm and an abrasion index (Ia) or wt% of powders with a particle size ≤0.5 mm. Additionally, and for comparative purposes, these indexes were also measured in cubes of commercial cordierite (Celcor® Corning Inc. 31 cells/cm^2) and the calcined (400 °C) epiphysis of a sheep humerus. This latter material has been selected as reference due to the potential application of the whey derived carbons in bone tissue engineering.

3. Results and discussion

Whey powder has particles of heterogeneous sizes between 10 μm and 200 μm (Fig. 1). Statistical analysis carried out on SEM images determined that the mode particle size was 20 ± 5 μm.

These particles are composed mainly of C, O and H, with also a relatively important amount of N (Table 1). In terms of composition, including ash content, and pH, the whey powder used in this work is representative of sweet wheys, i.e., those obtained in the production of cheese [23,25,26]. Ash is mainly constituted of K and P.

The process for producing the 3-D structured porous carbon described in this work involves the carbonisation of whey powders confined in a mould, at atmospheric pressure. Results obtained were certainly surprising as the resulting carbon materials showed an unexpected mechanical stability. Fig. 2 shows a variety of carbon pieces that are intended as examples of the potential that these new carbons could have in many different applications. The outer surfaces of the pieces were relatively smooth and glossy, free of cracks. Moreover, the mechanical consistence of these hard carbons was enough to withstand mechanisation with abrasive tools, as shown in Fig. 2d.

Carbons obtained from whey powders are very different to those prepared either from powdered carbohydrates (lactose) or whey protein isolates under identical conditions. Fig. 3 shows the outcomes of the carbonisation of powders that were poured in identical ceramic crucibles and pre-treated in air for 2 h and then placed, without demoulding, in the tubular oven under nitrogen (see Experimental section). The volatile emission in both systems leads to foamy materials with very low mechanical resistance. The key factor that would explain the difference between the behaviour of the three precursors, from a microscopic point of view, is the sintering of the whey powder particles.

The word “sintering” is used here to explain the inter-particle fusion that was observed by SEM (Fig. 4). The particle fusion seems to be restricted to the skin of the whey spheres inasmuch as the shape of those original spheres (Fig. 1) is still resembled in the micrographs of carbons obtained at high temperatures (Fig. 4). This phenomenon is, to our knowledge, the first time that is observed in the carbonisation process of a biomass precursor and resembles the partial melting of the phenolic resin particles described in detail in the landmark work of Tennison [19].

The sintering of the whey powders was found to occur at temperatures as low as 120-150 °C. At 120 °C or below, the pieces conformed tend to disaggregate when handled. 150 °C was found to be the minimum temperature that guaranteed the integrity of the conformed structure for further use. Two fundamental corollaries to this sintering process must be pointed out. First, no melting of whey was observed during the whole synthesis. Second, once the whey was conformed at a relatively low temperature (150 °C), the shape of the piece was preserved upon further heating under N_2 atmosphere. In this sense, the 3-D structured carbons shown in Fig. 2 were first pre-conformed by heating whey powders confined in a mould up to 150 °C, under atmospheric pressure. The pieces were then demoulded and carbonised (at 800 °C, in these particular examples) in an inert atmosphere of N_2, also in absence of external overpressure. As already stated in the Experimental Section, it should be clear, though, that whey derived carbons can be obtained by direct, one-step carbonisation from room to the desired temperature.

We think the two-step synthesis offers several advantages over the one-step carbonisation. Thus, relatively low temperature bearing moulds (i.e., silicone moulds) can be used to shape the

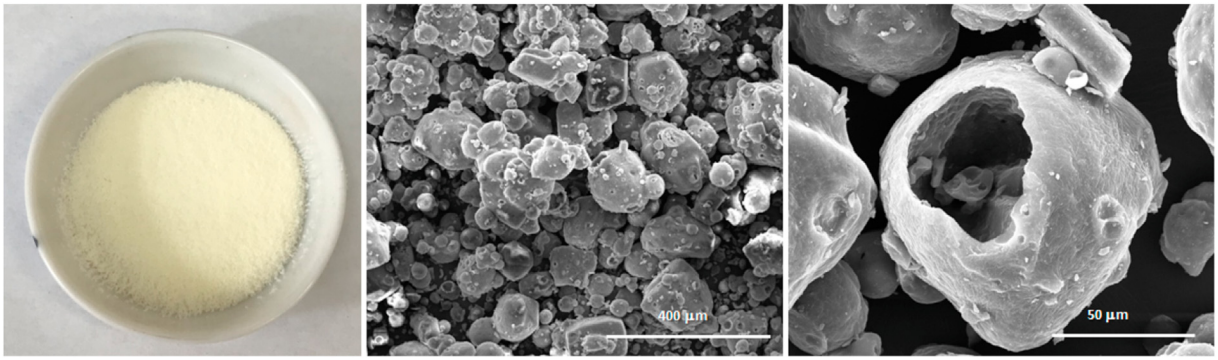

Fig. 1. Physical aspect (left) and SEM microphotographs of the whey powder.

Table 1
Composition, elemental analysis and pH of the whey powder.

Main components[a] (wt%)		Element[b] (wt%)	
Carbohydrate (lactose)	78.4	**C**[c]	40.7
Protein	12.7	**H**[c]	6.3
Fat	1.8	**N**[c]	2.3
Ash	4.4	**O**[c]	46.1
Moisture	2.7	**S**[c]	0.2
pH_{sat}[f]	5.1	**Na**[d]	0.3
		K[d]	1.2
		Mg[d]	0.1
		Ca[d]	0.4
		P[d]	0.6
		Cl[e]	0.2

[a] Supplier specifications.
[b] Dry basis.
[c] Organic (CHNSO) elemental analysis.
[d] ICP-MS.
[e] Chloride ISE.
[f] pH of a whey powder saturated solution.

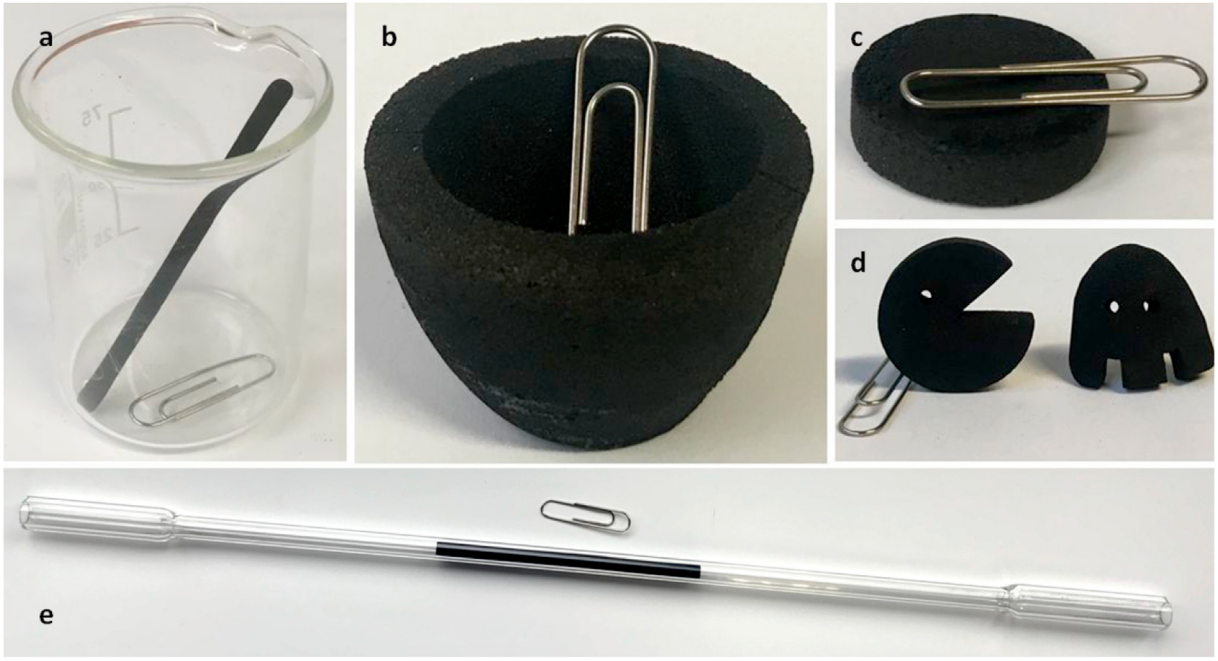

Fig. 2. Different pieces obtained by casting of whey powders: (a) rod, (b) crucible, (c) disc, (d) pieces that were prepared by mechanisation of two discs, (e) jacketed rod.

carbons. Also, due to the relatively mild conditions of the pre-conforming process (150 °C, 2 h), the initial atmosphere can be either N_2 or air with no significant changes observed in the physicochemical properties of the carbon materials resulting after the carbonisation process. Moreover, the yield of the pre-conforming step was identical under both atmospheres. This is a relevant observation since it differs from the behaviour of other carbon precursors that require a curing/crosslinking step prior carbonisation [6]. Finally, it is also noticed that the two-step sintering mechanism proposed here opens the door to more complex shapes by additive manufacturing with whey powders.

The materials pre-conformed at 150 °C had the characteristic colour resulting from non-enzymatic browning. As the carbonisation progressed, the emission of volatiles was accompanied by a considerable shrinkage of the initial pieces. Fig. 5 shows the volume reduction calculated over prismatic structures (see picture on top), and the variation of the yield with the carbonisation temperature.

The volume reduction of the sample HW150, heated in air at 150 °C, was negligible. The yield of the pre-conformed process was almost 95%, essentially due to the loss of moisture. However, the sample carbonised at 450 °C underwent a contraction of about 50% of its original volume and an important yield reduction, down to 38 wt%. Further reduction of yield was observed at 850 °C (32 wt% of yield), with little but consistent variation from that temperature on up to 1000 °C. Shrinkage behaviour was slightly different with an important decrease of the original volume observed at 450 °C and 750 °C then remaining constant, within experimental error, up to 1000 °C.

Results of the compositional analysis of the whey-derived carbons obtained at different temperatures are collected in Table 2. The C content only increased 6% from 450 °C to 1000 °C, suggesting that carbonisation of whey is almost completed at temperatures ca. 500 °C as also supported by the yield results of Fig. 5. The volatile emission during carbonisation encompassed the concentration of

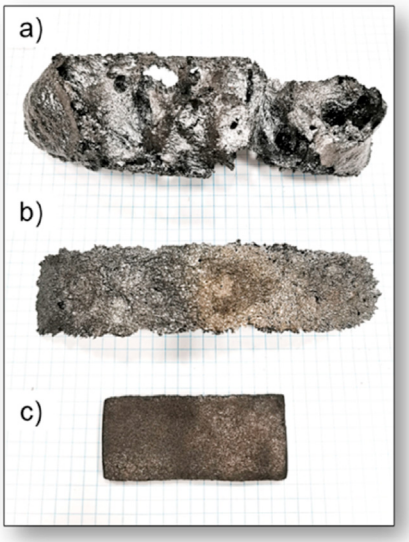

Fig. 3. Carbons obtained after the carbonisation of 5 g of a) lactose, b) whey protein isolate (WPI) and c) whey powder at 800 °C. All experiments were carried out in ceramic crucibles under identical heating conditions. (A colour version of this figure can be viewed online.)

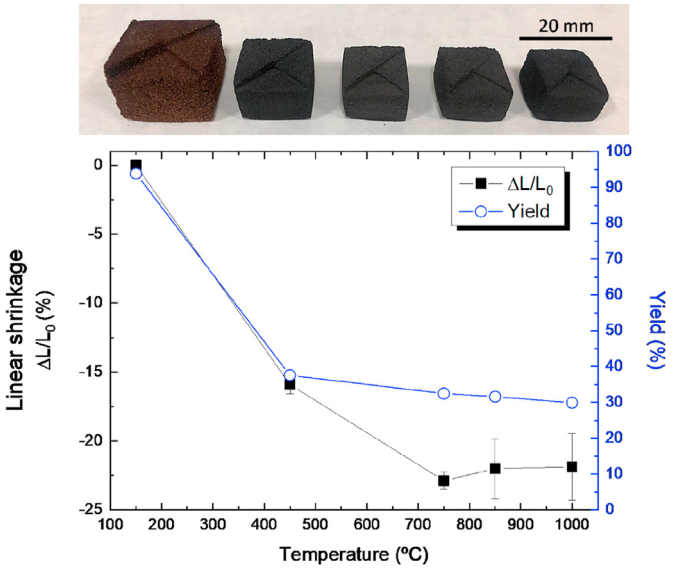

Fig. 5. Variation of the linear shrinkage (%) and yield (%) of whey-derived carbons with the carbonisation temperature. The linear shrinkage was equivalent in all three directions of the prisms. (A colour version of this figure can be viewed online.)

ashes in the carbon materials. The ash content of the carbons would be also responsible of their high basicity, as revealed by their high pH_{pzc}. Also ashes remaining in the carbons would explain the relatively high moisture values found even for carbons obtained at 1000 °C. The relatively high ash content of the whey-derived carbons would certainly limit their application in, for example, electrochemical devices. It should be noted here that a significant amount of the ashes (ca. 40%) could be removed by a gentle washing with cold water, rendering carbons with ash contents of approx. 8.5%. This content could be acceptable in industrial applications as those mentioned in the Introduction, i.e., gas filters, catalysts supports, etc. For applications demanding 3-D structured carbons with very low ash contents, it is envisaged that, in addition to conventional acid washing, desalted whey powders would be a feasible alternative (but obviously at a cost).

The characterisation of the porosity of the whey-derived carbons included conventional techniques for the analysis of pores of

Table 2
Elemental analysis, moisture, ash content and pH_{pzc} of the whey-derived carbons obtained at different carbonisation temperatures.

(wt%)	PW450	PW750	PW850	PW1000
C[a]	70.9	74.3	75.2	76.1
H[a]	3.2	1.1	0.8	0.6
N[a]	3.6	3.0	2.5	2.0
O[a]	14	13.6	12.4	11.2
S[a]	0.2	0.1	0.1	0.1
Moisture	7.4	9.3	10.1	8.9
Ash[a]	11.3	13.6	12.5	13.7
pH_{pzc}	10.4	11.3	11.1	10.6

[a] Dry basis.

different size. Starting with N_2 adsorption at −196 °C, Fig. 6 shows the adsorption-desorption isotherms on the different carbons. Temperature treatments up to 800 °C brought about non-porous materials, as measured with this technique (the isotherm of

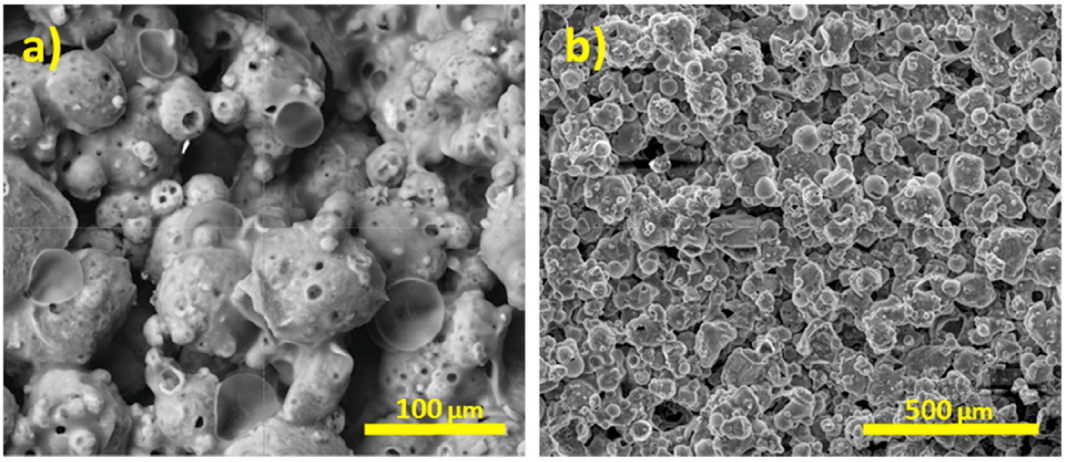

Fig. 4. SEM microphotographs of carbons obtained from the sintering of whey powder at different temperatures, a) PW850; b) PW1000. (A colour version of this figure can be viewed online.)

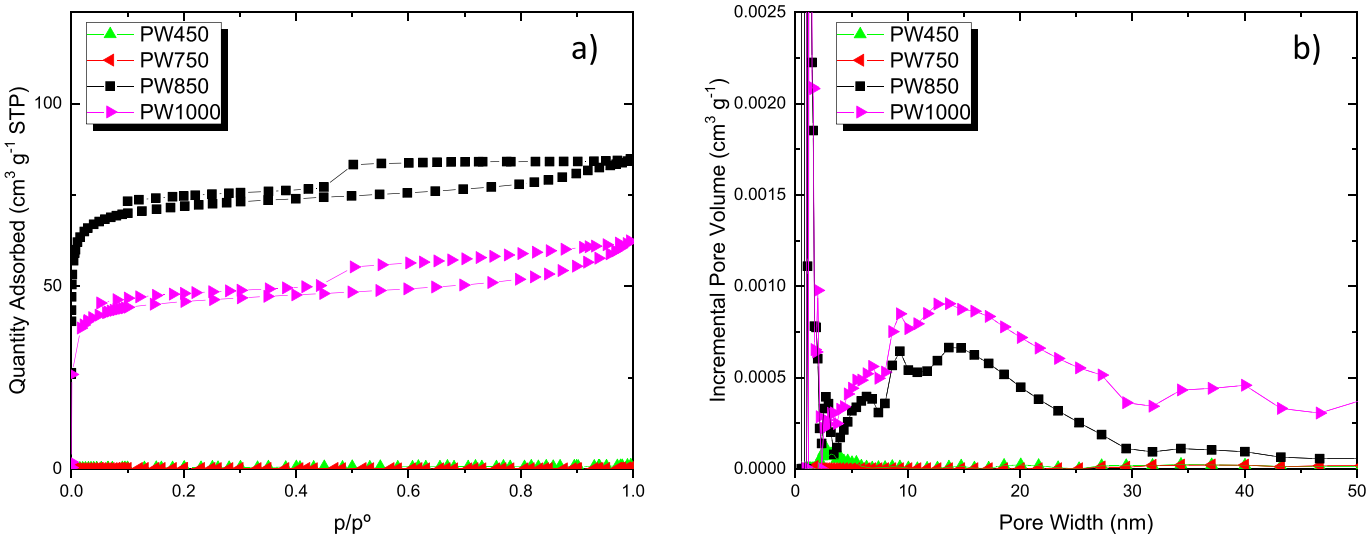

Fig. 6. a) N_2 adsorption isotherms (−196 °C) of four whey-derived carbons; b) DFT PSDs of the same carbons. (A colour version of this figure can be viewed online.)

PW800 is not shown here but it is similar to that of PW750, i.e., the material does not adsorb N_2 at −196 °C). Materials prepared at higher temperatures, i.e., PW850 adsorbed significant quantities of N_2 at cryogenic conditions. The isotherm of this carbon is type IV, which is characteristic of materials combining micro and mesoporosity. The same type of isotherm was obtained on PW1000, although a significant decrease of the porosity is already observed with respect to PW850. The non-closing hysteresis loops are characteristic of chars and indicate diffusion limitations during N_2 adsorption. Pore size distributions (PSDs) of both samples are shown in Fig. 6b, with mesopores centred at ca. 14 nm. Some relevant textural parameters of the samples are collected in Table 3. The porosity of PW850 and PW1000 samples, as tested by N_2 adsorption at −196 °C, is quite modest, with S_{BET} values well below that of conventional activated carbons (ca. 1000 m^2g^{-1}). Still, the presence of this incipient micro and mesoporosity anticipates the possibility of further activation of these materials. This possibility is out of the scope of this paper and will be investigated (and reported) in due course.

Macropores are conspicuous in the SEM images of the whey-derived carbons presented so far (see, for example, Fig. 4). Hg intrusion experiments exposed a wide macroporous network with maxima at 25–33 μm for carbons prepared at temperatures ≥450 °C (Fig. 7 and Table 3). This technique was also sensitive in detecting the progressive densification of the 3-D carbons with temperature. Real (He) densities also increased with temperature up to 850 °C, with a further heating up to 1000 °C showing no influence in that parameter. As a consequence, there was a significant decrease of the porosity of PW1000 when compared with either PW850 or PW750. As shown in Fig. 7, most of this porosity loss was attained at the expense of the pore contraction on both sides of the PSD distribution, i.e., both wide macropores and small macro/wide mesopores disappear after the highest temperature treatment. It is finally pointed out that were geometric densities (i.e., mass over geometric volume of the pieces) used in the porosity calculation instead of ρ_{Hg}, the porosity of PW1000 would have been identical to

Table 3
Porous properties of the whey-derived carbons[a].

SAMPLE	S_{BET}[a] (m^2/g)	V_p[a] (cm^3/g)	V_{micro}[a,b] (cm^3/g)	V_{meso}[a] (cm^3/g)
PW450	<10	–	–	–
PW750	<10	–	–	–
PW850	286	0.131	0.113	0.018
PW1000	181	0.097	0.074	0.023

	V_{meso}[c] (cm^3/g)	V_{macro}[c] (cm^3/g)	dp[c,d] (μm)	ρ_{Hg}[c] (g/cm^3)	ρ_{He}[e] (g/cm^3)	Porosity[f] (%)	V_T[g] (cm^3/g)
PW450rowhead	0.053	1.491	33.3	0.78	1.61	52	1.544
PW750rowhead	0.036	1.401	27.7	0.80	1.91	58	1.437
PW850rowhead	0.025	1.469	27.1	0.85	2.06	59	1.607
PW1000rowhead	0.027	1.109	25.3	1.06	2.04	48	1.21

Cubes (1 cm edge length) were ground to <1 mm particles to carry out the N_2 adsorption experiments. Hg intrusion experiments were carried out using small pieces (rectangular prisms of approx. 0.8 × 0.3 cm sides).

[a] N_2 isotherm.
[b] Dubinin-Radushkevich.
[c] Hg intrusion.
[d] maxima of the Hg PSD
[e] He intrusion.
[f] Porosity = $[1-(\rho_{Hg}/\rho_{He})]\times100$.
[g] $V_T = V_{micro}^{a,b} + V_{meso}^{c} + V_{macro}^{c}$.

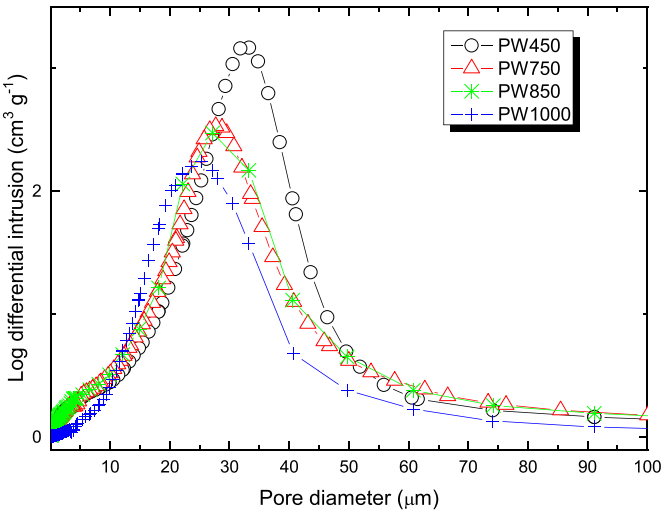

Fig. 7. Macropore size distributions of the whey-derived carbons as measured by Hg intrusion. (A colour version of this figure can be viewed online.)

that of PW850 (Fig. 5).Fig. 7.

In addition to the characterisation of the porosity, the permeability of rods of whey-derived carbons prepared at different temperatures was measured. Since the permeability throughout the 3-D structured carbons is governed by large, interconnected macropores, the differences found between samples carbonised at different temperatures were minimal, varying from 0.5 to 1×10^{-12} m^2. The permeability values of these novel 3-D structured porous carbons are very close to that of porous carbons prepared from powders of phenolic resins with mean particle size between 50 and 200 μm [19].

So far, it has been demonstrated that whey-derived carbons are hierarchical porous materials. The special relevance of these materials lays, as mentioned in the Introduction, on their outstanding mechanical properties. Standard flexural studies indicated a brittle, ceramic-like behaviour for all samples tested (Fig. 8a). Average flexural strength and modulus of the whey-derived carbons are shown in Fig. 8b. Both flexural properties increased steadily with the carbonisation temperature, following the densification of the structures (Table 3). Maximum values were thus obtained for sample PW1000, with a flexural strength comparable to that of 3-D structured resin-derived porous carbons (Fig. 9) [34,35]. Moreover, the flexural parameters of the whey derived carbons are within the range of values corresponding to human trabecular bones [36], thus opening the possibility of application of these whey-derived carbons as scaffolds for tissue engineering [37]. It is expected that the use of external overpressure either in the pre-conforming step and/or during the carbonisation would render less porous materials but with enhanced flexural properties.

An additional mechanical characterisation of the whey-derived carbons was devoted to measure their abrasion resistance. This parameter is very relevant, for example, in industrial applications requiring packing elements or dealing with fluid currents containing solid particles. As shown in Fig. 10, results of the two abrasion indexes selected are impressive for the 3-D structures prepared. The cohesion index (Ic) increased with temperature up to PW850, thus suggesting that the integrity (shape) of the initial pieces was better maintained as the carbonisation temperature was ≥850 °C. The abrasion index (Ia), which gives an indication of the production of fine particles, decreased with temperature with no significant differences between the Ia values of PW850 and PW1000. The abrasion of the whey-derived carbons seemed to be related to the inner properties of the carbon particles rather than to the porosity of the 3-D structures (Table 3). Thus, the best performing materials (PW850 and PW1000) were those with higher He densities in spite of their high porosity values. Values of Ia and Ic of the whey-derived carbons were compared to those of two reference materials with a similar geometry, namely a commercial cordierite honeycomb used as a catalytic support, and a trabecular bone (the epiphysis of a sheep humerus) previously calcined at 400 °C. This latter reference material clearly underperformed in comparison with the whey-derived carbons.

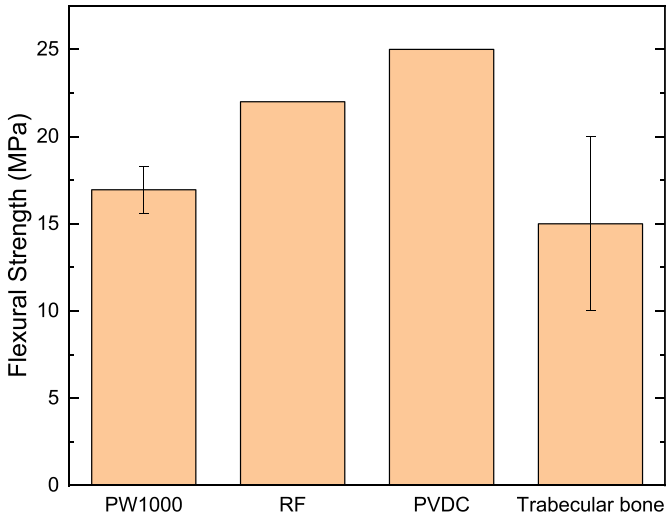

Fig. 9. Flexural strength of different 3-D structured porous carbons. Labels: PW1000, whey derived carbon; RF, porous carbon monolith prepared from resorcinol/formaldehyde [35]; PVDC, porous carbon monolith prepared from polyvinylidene chloride [36]; trabecular (cancellous) bone [37]. The error bar of the trabecular bone mean value intends to represent the span of flexural strengths of these bones, i.e., between 10 and 20 MPa [37][[38]]. (A colour version of this figure can be viewed online.)

The outstanding mechanical properties of these 3-D structured porous carbons were totally unexpected bearing in mind the carbonisation of disaccharides including sucrose and lactose (Fig. 3). The question that naturally arises is what makes whey powders, which are almost 80% lactose (Table 3), to behave so different. Most lactose in non-hygroscopic whey powders as those used in this

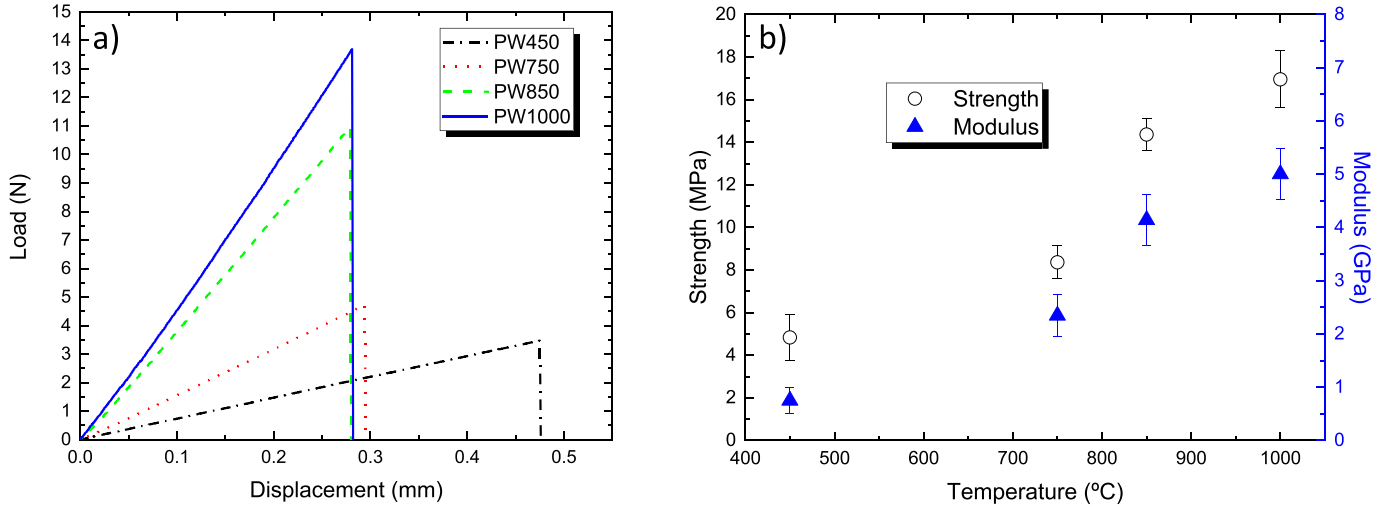

Fig. 8. a) Selected examples of the flexural tests carried out with whey-derived carbons; b) flexural strength and modulus of the whey-derived carbons prepared at different carbonisation temperatures. (A colour version of this figure can be viewed online.)

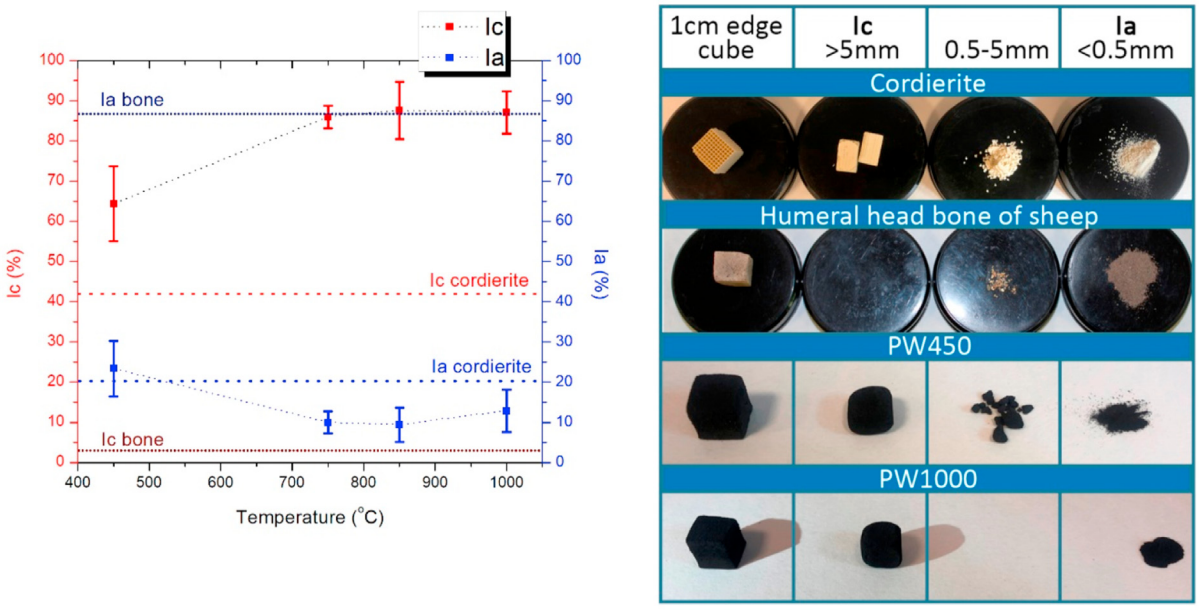

Fig. 10. Variation of the cohesion (Ic) and abrasion (Ia) indexes of cubes (1 cm edge) of whey-derived carbons with the temperature of carbonisation. Cordierite honeycomb and a cube cut from the epiphysis of the humerus of a sheep (both also 1 cm edge) were used as references (left); photographs of the results of the tests for PW450 and PW1000 and the monolith of cordierite and sheep bone carried out using the same test conditions (right). (A colour version of this figure can be viewed online.)

paper is present as crystalline α-lactose monohydrate [26]. Next in abundance in whey powder are whey proteins, mainly lactoglobulins. Thermogravimetric analysis (TG) of whey powder and those two main components (whey proteins as whey protein isolate or WPI) under carbonisation conditions (N_2 atmosphere) are shown in Fig. 11. There are significant differences between the weight loss profiles of the whey powder and those of lactose and WPI. In other words, the concurrence of proteins and lactose in whey alters significantly the volatile emission of the powder. In fact, volatiles evolved much earlier in whey powders, which exhibited a maximum DTG peak at 220 °C. This means that when lactose caramelisation reached its maximum (236 °C) the weight loss in whey powders almost doubled that of pure lactose. Whey proteins in the meantime experienced little weight loss apart from the initial moisture release.

Transformations that altered the pyrolysis of the whey powder from the expected "pure" lactose behaviour seem then to take place at early stages of the heating process. These transformations are most likely related to the possibility of obtaining mechanically consistent 3-D structures from whey powder. These structures are attained at temperatures between 120 and 150 °C through the sintering of the surfaces of the whey particles, as mentioned earlier. Whey particles are not homogeneous in composition. Previous studies have demonstrated that, due to diffusion restrictions during the spray drying process, proteins and fat tend to concentrate on the whey particle surfaces [39]. Reactions at those surfaces are thus

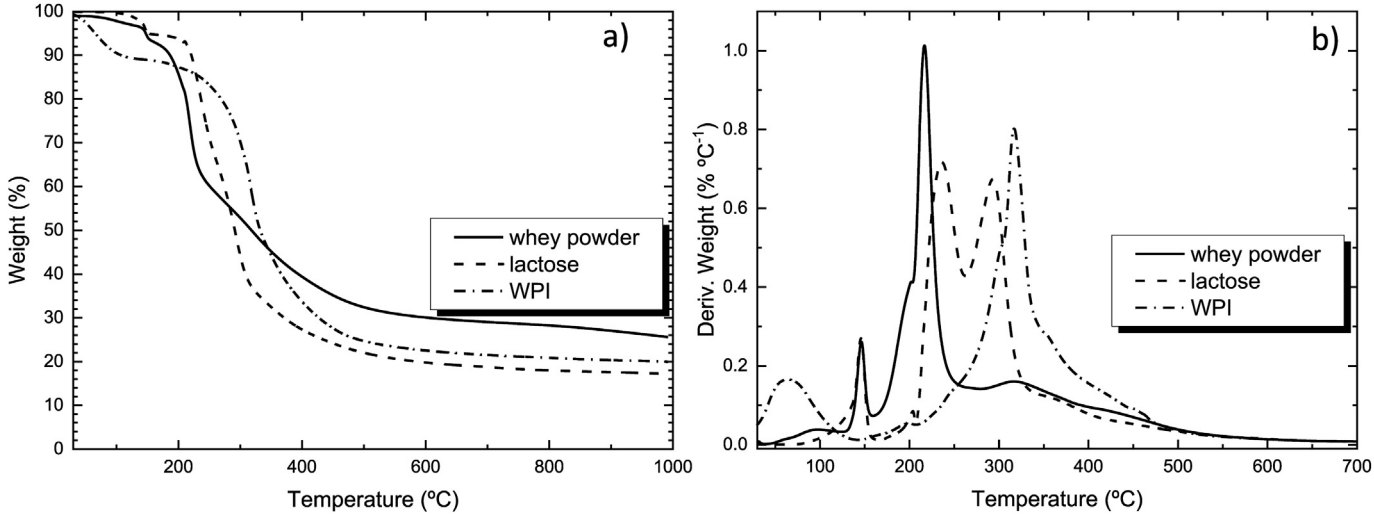

Fig. 11. a) TG and b) DTG profiles (in N_2) of whey powder, α-lactose monohydrate and a whey protein isolate (WPI). DTG temperature scale has been shortened to improve clarity.

far from those expected from a highly loaded lactose product.

Two possibilities are then proposed to explain the thermal behaviour of whey powders. First, the formation of melanoidins in the Maillard reaction between lactose and proteins. This family of reactions is expected to start at temperatures well below 100 °C, depending on a number of conditions including pH and water activity. This latter parameter would increase on the surface of the whey particles as the temperature approaches 150 °C, i.e., the temperature at which the loss of crystalline water of the α-lactose monohydrate occurs bringing about the first peak in the DTG profiles of both whey and pure lactose (Fig. 11). Formation of melanoidins could be then boosted when enough water is available on the surface of the particles. These melanoidins would soon decompose with the emission of volatiles and leaving a carbon residue that would keep the powder particles together.

Water would also play a fundamental role in the second type of plausible transformations that may occur at the surface of the whey particles –the thermal gelation of whey proteins. Whey proteins, specifically β-lactoglobulin, are globular proteins that unfold in water solutions at 60 °C. Once unfolded and as the temperature of the solution raises, the protein chains start to aggregate irreversibly to form a gel [40]. The proteins on the whey particles surfaces still maintain their natural structure in spite of the spray drying process [41]. As the temperature increases and crystallisation water from lactose becomes available, protein gels may originate on the surface of the particles acting as a glue to stick them.

These two possibilities would deliver a new type of macromolecules that would be absent during the pyrolysis of the single components. The formation of those macromolecules at relatively low temperatures (120-150 °C) would reduce the temperature at which the maximum evolution of volatiles occurs (Fig. 11). In addition, the sintering of the whey particles surfaces may limit the release of volatiles to intraparticle spaces, thus generating the highly macroporous structures observed. In that sense, it is expected that the particle size distribution of the whey powder could be relevant in the final properties of the carbons obtained. Some volatiles would remain in the whey particles whose emission at temperatures above 800 °C would develop the micro and mesoporosity of the resulting carbons. A more in depth study is needed to determine the effect of the relative proportion of the whey main components in the final properties of the resulting carbons.

4. Conclusions

A new type of green, 3-D structured porous carbons, which can be precast by sintering in absence of external overpressure and subsequent carbonisation of whey powder, has been described. The pieces of carbon can be obtained in virtually any shape and they are characterised by a porosity of 50–60% that comprises micropores, mesopores and macropores up to 400 μm; a high permeability; and a very high mechanical integrity, considering the biomass origin of the precursor and the porosity of the resulting materials. The flexural strength of these 3-D porous carbons is comparable to those of porous carbon monoliths prepared from polymeric resins. In addition, these carbon materials contains N in proportions up to 3 wt%. The mechanical properties of the whey derived carbons are totally unexpected from the performance of the two main single components of whey powders, namely lactose and whey proteins (β-lactoglobulin). Two tentative mechanisms including Maillard reactions and protein gel formation are proposed to explain such differences. These findings open new routes to obtain mechanically robust 3-D porous carbons from biomass.

CRediT authorship contribution statement

Raúl Llamas-Unzueta: Investigation, Visualization. **J. Angel Menéndez:** Conceptualization, Writing - original draft. **Luis A. Ramírez-Montoya:** Investigation, Visualization. **Jaime Viña:** Methodology, Validation, Writing - review & editing. **Antonio Argüelles:** Methodology, Validation. **Miguel A. Montes-Morán:** Investigation, Conceptualization, Writing - original draft.

Declaration of competing interest

The authors declare that they have no known competing financial interests or personal relationships that could have appeared to influence the work reported in this paper.

Acknowledgments

We thank financial support from the MINECO (Project CTQ2017-87820-R) and Principado de Asturias-FICYT-FEDER (Project PCTI-Asturias IDI/2018/000118). L.A. Ramírez-Montoya thanks CONACyT, México, for a post-doctoral grant (CVU No 330625, 2017). We thank Massimiliano Forlano (CAPSA FOOD) for the whey powder samples. We also thank Dr. Marbán for helping with the experimental He permeabilities.

References

[1] K.M. De Lathouder, E. Crezee, F. Kapteijn, J.A. Moulijn, Carbon monoliths in catalysis, in: P. Serp, J.L. Figueiredo (Eds.), Carbon Materials for Catalysis, John Wiley & Sons, New Jersey, 2009, pp. 401–428.
[2] A. Arami-Niya, T.E. Rufford, Z. Zhou, Activated carbon monoliths with hierarchical pore structure from tar pitch and coal powder for the adsorption of CO_2, CH_4 and N_2, Carbon 103 (2016) 115–124.
[3] A. Szczurek, V. Fierro, A. Pizzi, A. Celzard, Emulsion-templated porous carbon monoliths derived from tannins, Carbon 74 (2014) 352–362.
[4] L. Yu, N. Brun, K. Sakaushi, J. Eckert, M.M. Titirici, Hydrothermal nanocasting: synthesis of hierarchically porous carbon monoliths and their application in lithium–sulfur batteries, Carbon 61 (2013) 245–253.
[5] S.R. Sandeman, C.A. Howell, S.V. Mikhalovsky, G.J. Phillips, A.W. Lloyd, J.G. Davies, S.R. Tennison, A.P. Rawlinson, O.P. Kozynchenko, Inflammatory cytokine removal by an activated carbon device in a flowing system, Biomaterials 29 (2008) 1638–1644.
[6] T. Vergunst, M.J.G. Linders, F. Kapteijn, J.A. Moulijn, Carbon-based monolithic structures, Catal. Rev. 43 (2001) 291–314.
[7] J.M. Ramos-Fernández, M. Martínez-Escandell, F. Rodríguez-Reinoso, Production of binderless activated carbon monoliths by KOH activation of carbon mesophase materials, Carbon 46 (2008) 384–386.
[8] K.M. de Lathouder, J. Bakker, M.T. Kreutzer, F. Kapteijn, J.A. Moulijn, S.A. Wallin, Structured reactors for enzyme immobilization: advantages of tuning the wall morphology, Chem. Eng. Sci. 59 (2004) 5027–5033.
[9] A. Zhakeyev, P. Wang, L. Zhang, W. Shu, H. Wang, J. Xuan, Additive manufacturing: unlocking the evolution of energy materials, Adv. Sci. 4 (2017), 1700187.
[10] Y. Lakhdar, C. Tuck, J. Binner, A. Terry, R. Goodridge, Additive manufacturing of advanced ceramic materials, Prog. Mater. Sci. 116 (2021), 100736.
[11] C. Zhu, T.Y.-J. Han, E.B. Duoss, A.M. Golobic, J.D. Kuntz, C.M. Spadaccini, M.A. Worsley, Highly compressible 3D periodic graphene aerogel microlattices, Nat. Commun. 6 (2015) 6962.
[12] N. Yoshizawa, M.-M. Titirici, A sustainable synthesis of nitrogen-doped carbon aerogels, Green Chem. 13 (2011) 2428–2434.
[13] S.-A. Wohlgemuth, R.J. White, M.-G. Willinger, M.-M. Titirici, M. Antonietti, A one-pot hydrothermal synthesis of sulfur and nitrogen doped carbon aerogels with enhanced electrocatalytic activity in the oxygen reduction reaction, Green Chem. 14 (2012) 1515–1523.
[14] M. Taubert, J. Beckmann, A. Lange, D. Enke, O. Klepel, Attempts to design porous carbon monoliths using porous concrete as a template, Mic. Mes. Mat. 197 (2014) 58–62.
[15] A.B. Fuertes, G. Marbán, D.M. Nevskaia, Adsorption of volatile organic compounds by means of activated carbon fibre-based monoliths, Carbon 41 (2003) 87–96.
[16] J.M. Gatica, G.A. Cifredo, G. Blanco, S. Trasobares, H. Vidal, Unveiling the source of activity of carbon integral honeycomb monoliths in the catalytic methane decomposition reaction, *Cat*, Today Off. 249 (2015) 86–93.
[17] S. Gao, L. Ge, B.S. Villacorta, T.E. Rufford, Z. Zhu, Carbon monoliths by assembling carbon spheres for gas adsorption, Ind. Eng. Chem. Res. 58 (2019) 4957–4969.

[18] D. Lozano-Castelló, D. Cazorla-Amorós, A. Linares-Solano, D.F. Quinn, Activated carbon monoliths for methane storage: influence of binder, Carbon 40 (2002) 2817–2825.
[19] S.R. Tennison, Phenolic-resin-derived activated carbons, Appl. Catal., A 173 (1998) 289–311.
[20] V.I. Águeda, B.D. Crittenden, J.A. Delgado, S.R. Tennison, Effect of channel geometry, degree of activation, relative humidity and temperature on the performance of binderless activated carbon monoliths in the removal of dichloromethane from air, Separ. Purif. Technol. 78 (2011) 154–163.
[21] B. Crittenden, A. Patton, C. Jouin, S. Perera, S. Tennison, J.A.B. Echevarria, Carbon monoliths: a comparison with granular materials, Adsorption 11 (2005) 537–541.
[22] M. Kunowsky, A. Garcia-Gomez, V. Barranco, J.M. Rojo, J. Ibañez, J.D. Carruthers, A. Linares-Solano, Dense carbon monoliths for supercapacitors with outstanding volumetric capacitances, Carbon 68 (2014) 553–562.
[23] A.R. Prazeres, F. Carvalho, J. Rivas, Cheese whey management: a review, J. Environ. Manag. 110 (2012) 48–68.
[24] N. Venetsaneas, G. Antonopoulou, K. Stamatelatou, M. Kornaros, G. Lyberatos, Using cheese whey for hydrogen and methane generation in a two-stage continuous process with alternative pH controlling approaches, Bio Technol. 100 (2009) 3713–3717.
[25] J.G. Zadow, Whey and Lactose Processing, Elsevier, Essex, 1992.
[26] J.G. Zadow, Whey and Whey Powders-Production and Uses, Encyclopedia of Food Science and Nutrition, Elsevier, 2003, pp. 6147–6152.
[27] L.A. Pfaltzgraff, M. De bruyn, E.C. Cooper, V. Budarin, J.H. Clark, Food waste biomass: a resource for high-value chemicals, Green Chem. 15 (2013) 307–314.
[28] R. Ravindran, A.K. Jaiswal, Exploitation of food industry waste for high-value products, Trends Biotechnol. 34 (2016) 58–69.
[29] Y. Li, H. Liu, K. Xiao, X. Liu, H. Hu, X. Li, H. Yao, Correlations between the physicochemical properties of hydrochar and specific components of waste lettuce: influence of moisture, carbohydrates, proteins and lipids, Bio Technol. 272 (2019) 482–488.
[30] H.-B. Chen, Y.-Z. Wanga, D.A. Schiraldi, Foam-like materials based on whey protein isolate, Eur. Polym. J. (2013) 3387–3391.
[31] M. Koller, R. Bona, E. Chiellini, E.G. Fernandes, P. Horvat, C. Kutschera, P. Hesse, G. Braunegg, Polyhydroxyalkanoate production from whey by Pseudomonas hydrogenovora, Bio Technol. 99 (2008) 4854–4863.
[32] M. Wahid, G. Parte, D. Phase, S. Ogale, Yogurt: a novel precursor for heavily nitrogen doped supercapacitor carbon, J. Mater. Chem. 3 (2015) 1208–1215.
[33] M. Escala, A. Graber, R. Junge, C.H. Koller, V. Guiné, R. Krebs, Hydrothermal carbonization of organic material with low dry matter content: the example of waste whey, J. Residuals Sci. Technol. 10 (2013) 179–186.
[34] J.A. Menéndez, M.J. Illán-Gómez, C.A. León y León, L.R. Radovic, On the difference between the isoelectric point and the point of zero charge of carbons, Carbon 33 (1995) 1655–1659.
[35] G. Hasegawa, K. Kanamori, T. Kiyomura, H. Kurata, T. Abe, K. Nakanishi, Hierarchically porous carbon monoliths comprising ordered mesoporous nanorod assemblies for high-voltage aqueous supercapacitors, Chem. Mater. 28 (2016), 3944–395.
[36] M.A. Wójtowicz, E.P. Rubenstein, M.A. Serio, J.E. Cosgrove, High-strength Porous Carbon and its Multifunctional Applications, US Patent US8615812 B2, 2013.
[37] Q. Fu, E. Saiz, M.N. Rahaman, A.P. Tomsia, Bioactive glass scaffolds for bone tissue engineering: state of the art and future perspectives, Mater. Sci. Eng. C 31 (2011) 1245–1256.
[38] H. Liu, L. Xia, Y. Dai, M. Zhao, Z. Zhou, H. Liu, Fabrication and characterization of novel hydroxyapatite/porous carbon composite scaffolds, Mater. Lett. 66 (2012) 36–38.
[39] P. Fäldt, B. Bergenståhl, Spray-dried whey protein/lactose/soybean oil emulsions. 1. Surface composition and particle structure, Food Hydrocolloids 10 (1996) 421–429.
[40] M. Verheul, S.P.F.M. Roefs, Structure of whey protein gels, studied by permeability, scanning electron microscopy and rheology, Food Hydrocolloids 12 (1998) 17–24.
[41] C. Vega, Y.H. Roos, Spray-dried dairy and dairy-like emulsions-compositional considerations, J. Dairy Sci. 89 (2006) 383–401.